

## **Atmospheric Neutral Density Experiment Mission Update**

**A. Nicholas, G. Gilbreath, S. Thonnard, I. Galysh, L. Healy, L. Wasiczko, R. Burris**

*Naval Research Laboratory*

**T. Finne**

*Praxis, Inc.*

**M. Davis**

*Honeywell TSI*

**B. Bruninga**

*US Naval Academy*

**D. Hall**

*Boeing LTS, Inc.*

**P. Kervin**

*Air Force Research Laboratory*

### **ABSTRACT**

The Atmospheric Neutral Density Experiment (ANDE) Risk Reduction flight was launched on Dec. 9, 2006 and deployed into orbit by the Space Shuttle Discovery on Dec. 21, 2006. The primary mission objective is to test the deployment mechanism from the Shuttle for the ANDE flight in mid 2009. Scientific objectives of the ANDE risk reduction flight include; monitor total neutral density along the orbit for improved orbit determination of resident space objects, monitor the spin rate and orientation of the spacecraft, provide a test object for polarimetry studies using the HI-CLASS system.

Each of the two ANDE missions consists of two spherical spacecraft fitted with retro-reflectors for satellite laser ranging (SLR). The ANDE risk reduction mission spacecraft each contain a small lightweight payload designed to determine the spin rate and orientation of the spacecraft from on-orbit measurements and from ground based observations. The follow-on ANDE mission scheduled for launch in 2009 will consist of two spherical spacecraft also fitted with retro-reflectors for SLR. One of these spacecraft will also carry instrumentation to measure the in-situ atmospheric density, composition and winds.

This paper presents a mission overview and emphasis will be placed on the scientific results from the risk reduction mission and a brief overview of the follow-on mission.

### **1. INTRODUCTION**

Significant advances in the miniaturization of space technology and cost reduction has supported the proliferation of micro satellites. Where once a single satellite contained a suite of instruments to support several mission objectives, often times not all related, current micro satellites are tailored to accomplish a small set of related objectives. Through the use of micro satellite technology, NRL is developing a satellite suite to improve precision orbit determination and prediction by monitoring total atmospheric density between 300 and 400 km. The suite, known as the Atmospheric Neutral Density Experiment (ANDE) [1,2], consists of a series of four micro satellites with instrumentation to perform these interrelated mission objectives. First, provide high quality satellites, with stable and well-determined coefficient of drag, for calibrating techniques and models for precision orbit determination. Second, provide detailed atmospheric composition for validating new ultraviolet remote sensing techniques. Finally, an optical communications experiment using modulating retroreflectors (MRRs) will be conducted during the ANDE mission. The DoD Space Test Program will provide launch services and deployment into orbit for two missions, each mission flying a pair of ANDE spacecraft. The ANDE risk reduction (ANDERR) mission was launched on Dec. 9, 2006 onboard STS-116, Space Shuttle Discovery, and deployed (as seen in Fig. 1) into orbit on Dec. 21, 2006. This paper will focus on the Atmospheric Neutral Density Experiment Risk Reduction (ANDERR) [3] flight, which consists of two spherical spacecraft with retro-reflectors for satellite laser ranging (SLR).

The constant and well-determined cross section and surface properties of the ANDERR spacecraft provide an ideal

set of objects for monitoring atmospheric drag. While the exterior of the ANDERR spacecraft determine how well the main science objective is accomplished nothing prohibits the use of the spacecraft's interior space. The interior can be utilized for additional experiments and payloads so long as the interior masses are balanced so that the center



Fig. 1. Deployment of ANDERR during STS-116 on Dec. 21, 2006. From bottom to top the objects are: the ICU lower cylinder ( 29663, with MAA spacecraft (29664) still inside), the ICU avionics deck (29666), the FCal spacecraft (29667), and the ICU upper cylinder (29665).

of gravity remains at the geometric center. Each of the four spacecraft has their interior populated differently to accommodate respective science goals. One spacecraft in the ANDE mission (launch in 2009) will contain instrumentation to measure the neutral and ion composition directly while the other spacecraft contain the subsystems necessary to measure and/or derive the secondary science objectives.

The primary mission of the ANDE program is to accurately determine the total atmospheric density along the orbit of the spacecraft. The major source of error in determining the orbit of objects in Low Earth Orbit (LEO), altitudes less than 1000 km, is the computation of acceleration due to atmospheric drag. This acceleration is governed by the equation,

$$a = -\frac{1}{2} B \rho v^2 \quad (1)$$

where  $a$  is the acceleration,  $\rho$  is the atmospheric density and  $v$  is the orbital velocity relative to the medium. The ballistic coefficient [4],  $B$ , is given by

$$B = \frac{C_D A}{m} \quad (2)$$

with  $C_D$  being the coefficient of drag,  $A$  the projected frontal area and  $m$  the mass of the object. The ANDERR spacecraft  $C_D$  values were modeled; the MAA average value is 2.1123 and the FCal average value is 2.1113 [5].

Several atmospheric density models are routinely used in orbit determination. These include the Jacchia 1970, J70, empirical model derived from satellite observations [6], the Mass Spectrometer Incoherent Scatter Radar Extended, MSISE-90, model [7,8] and the recently revised NRLMSISE-00 [9], hereafter referred to as MSIS. The quantity measured with this method is the product of the ballistic coefficient and the total atmospheric density. Hence, to retrieve atmospheric densities from orbital observations one must have adequate knowledge of the ballistic coefficient and the relative velocity of the object with respect to the medium. For example, consider a sphere of known mass in LEO. The cross-sectional area of a sphere is independent of orientation and is therefore constant. Assume the sphere does not have an attitude control system that requires thrusters; therefore the sphere's mass is constant. A high fidelity  $C_D$  model can be used to compute the  $C_D$  of the sphere for different conditions the sphere

will experience in orbit. Inputs to such a model consist of the properties of the surface material of the sphere, surface roughness, the temperature of the sphere, and the temperature and composition of the atmospheric constituents impinging the surface of the sphere [10,11]. The velocity of the sphere can be obtained from the orbit determination and the velocity of the atmosphere can be modeled using an atmospheric wind model such as the Horizontal Wind Model (HWM) [12].

## 2. SPIN RATE DETERMINATION

Due to a complication with the deployment apparatus the initial spin rate of the MAA spacecraft was not directly measured by on-board video from the Space Shuttle Discovery. The spin rate of the MAA spacecraft was estimated by several different methods; video from the STS-116 deployment, on-board telemetry from the MAA spacecraft, observations from the AEOS telescope on Maui, and satellite laser ranging (SLR) observations.

### 2.1 STS-116 Video and Still Analysis

The ANDERR spacecraft were launched on board the Space Shuttle Discovery on Dec. 9, 2006. The deployment of the spacecraft from the internal cargo unit (ICU) [3] occurred on Dec. 21, 2006 at 13:23:40 UT. The MAA spacecraft was expected to have approximately 5 rpm spin imparted by the deployment system. Video from the mission indicated that the MAA spacecraft did not immediately separate from the ICU cylinder, it remained inside the ICU (lower left object in Fig. 1). Photographs taken from the Space Shuttle Discovery 30 minutes after ANDERR deployment show the MAA emerging from the ICU cylinder as seen in Fig. 2 and Fig. 3. Fig. 4 shows the five distinct objects in a single scene.



Fig. 2. MAA emerges from ICU



Fig. 3. MAA emerges from ICU



Fig. 4. Photograph showing all five ANDERR deployables.

An analysis of the deployment video was performed to determine the spin rate of the lower ICU cylinder (containing the MAA spacecraft). The crosshair pattern on the bottom of the ICU was used as a reference to determine the spin rate. The ICU was observed to rotate 64 degrees in 30 seconds (Fig. 5 and 6), indicating to a maximum spin rate of approximately 0.35 rpm for the MAA/ICU system.



Fig. 5. ICU at t = 30 seconds



Fig. 6. ICU at t = 60 seconds

## 2.2 MAA Telemetry

An analysis was performed on the temperature data from the sensors located within the ½ inch thick shell of the spacecraft to determine the rotation rate of the MAA spacecraft. Twenty-seven days of data starting on Jan 1, 2007 were analyzed for this investigation. For each day, the onboard photovoltaic current and temperature telemetry was assessed. For each packet, the UT, local time, and location of the contacting site were identified. Knowledge of the local time at the HAM radio telemetry ground-site, allows one to calculate the sun orientation with respect to the MAA spacecraft at that point in time. Thermal data from the +X sensor in the spacecraft was analyzed and fit with a sinusoid. This fit is presented in Fig. 7 for data from January 24, 2007, which indicates that the +X face experienced thermal cycling (suggesting that it was rotating in and out of sunlight) with a period of approximately 6 minutes, corresponding to a spin rate of approximately 0.17 rpm. The data used to form this conclusion was one of the longest consistent data sets over a ground station in the 27-day data, and seemed to offer the most potential for analysis.

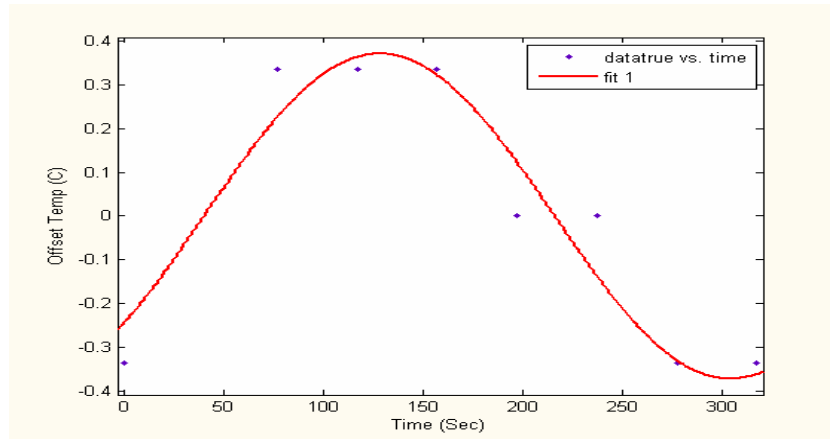


Fig. 7. Temperature telemetry analysis from Jan. 24, 2007

## 2.3 AEOS Observations

Photometric observations of the ANDE MAA spacecraft were acquired by the VISIM instrument of the AMOS AEOS telescope during a terminator pass on March 3, 2007 (05:54-05:59 UT). As shown in Fig. 8, AEOS acquired the satellite in sunlight and tracked it well into Earth shadow, through the entire penumbra and for  $\approx 1$  min into umbra. The faint in-umbra brightness is likely due to the satellite's retro-reflectors reflecting man-made Maui/Hawaii light back toward the telescope ("Maui Shine").

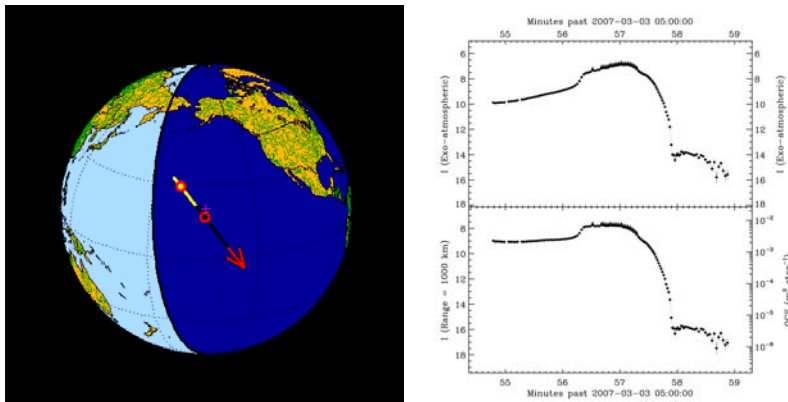


Fig. 8. The pass-geometry ground-track plot (left) and the measured calibrated I-band (725-925 nm) magnitudes (right) for the AEOS observation of the ANDE MAA sphere (SSN 29664) conducted 2007 Mar 03 (day of year 062).

During the early fully-sunlit portion of the pass, one upward brightness modulation is apparent (at 05:56:20) indicating that AEOS detected sunlight reflected from both dark and bright portions of the beach-ball satellite. The lowest panel of the right plot in Fig. 8 shows that this one observed modulation corresponded to a brightening from 9.0 stellar magnitudes up to 7.8 stellar magnitudes (range normalized to 1000 km). As explained below, to reproduce these observed brightness levels using a photometric model of the beach-ball satellite requires a bright-area albedo (i.e., reflectance) of  $0.76 \pm 0.10$  and a dark-area albedo of  $0.22 \pm 0.05$ .

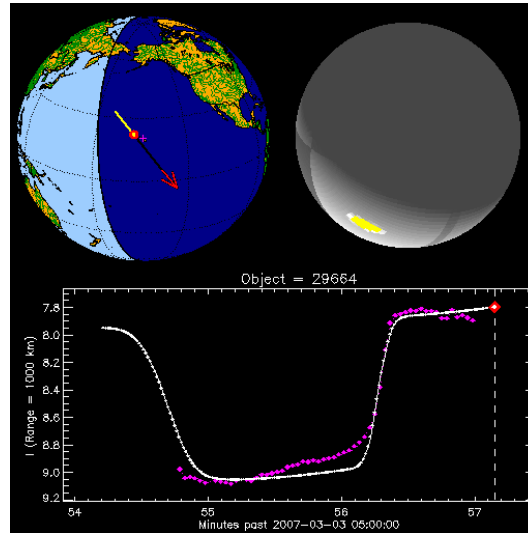


Fig. 9. Photometric model analysis of the ANDE MAA using the AEOS 2007 Mar 03 observations. The pink curve depicts the observations and the white curve the simulation using a 0.1 rpm spin rate.

An analysis was performed on the AEOS data to constrain the MAA spin rate as much as possible from the single observed brightness modulation (see Fig. 9). The white curve in Fig. 9 represents the signature from a simulated MAA spacecraft rotating at 0.1 rpm with bright-area albedos of 38% specular + 38% diffuse, and dark-area albedos of 11% specular + 11% diffuse, plotted over the observed data (pink curve). The data are consistent with these albedos because the upper and lower envelopes of the white and pink curves match during the fully sunlit portion of the pass (which lasted until approximately 05:57:30 UT). The spin-rate of 0.1 rpm is barely consistent with the data: any faster spin rate would have been detectable in the observations. However, the model plotted as the white curve in Fig. 9 assumes a simulated MAA spin-axis pointing at  $\text{DEC} = 90^\circ$ , which is just one possibility. Other assumptions for spin-axis orientation indicate similar albedos, but maximum spin-rates varying between 0.1 rpm and 0.2 rpm for the cases examined. Considering the sparse AEOS data (reliable spin rate determinations generally require many brightness modulations) and the unknown spin-axis orientation, a conservative interpretation of this single-pass observation indicates an upper-limit of 0.3 rpm for the MAA spin rate.

## 2.4 SLR Observations

The International Laser Ranging Service (ILRS) [13] performed satellite laser ranging observations of the ANDERR spacecraft. On April 16, 2007, satellite laser ranging data was acquired from the ILRS site located in Graz, Austria, as shown in Fig. 10. The data shows 4 retro reflectors coming into and out of view over a 3 minute 33 second period. An analysis of the spacing between each retro's closest approaches (valley of the "V") determined that the observations had spacings of .892, 1.0, and .788 (normalized to the longest span). A comparison with mechanical data of the MAA spacecraft revealed that these normalized spacing (1.0) corresponded with physical dimension of 7.837 inches. During the SLR observations it took 51 seconds to rotate through that distance, resulting in a rate of 0.12 rpm. However, during the pass the aspect angle to the spacecraft changed in azimuth by about  $135^\circ$ , resulting in an adjustment of 0.09 rpm. This adjustment should be added to or subtracted from the actual spacecraft spin rate to get the observed spin rate of 0.12 rpm.

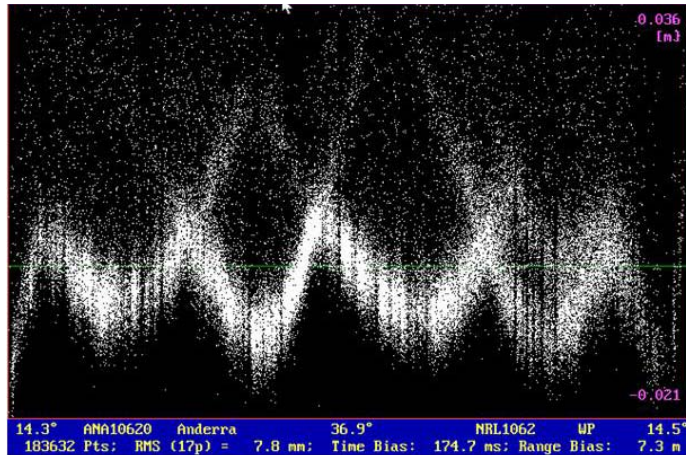


Fig 10. Laser Ranging Data from Graz, Austria; courtesy of Georg Kirchner and the ILRS.

As a result, depending on the direction of spin prograde or retrograde, the actual spacecraft rotation rate would appear to be bounded on the upper end by 0.21 rpm and on the lower end of 0.03 rpm. We would assume the latter, since it is doubtful that ANDERR MAA could actually speed up its spin in orbit above the January 24<sup>th</sup> and March 3<sup>rd</sup> observations of 0.17 and .10 respectively, and would more likely continue to slow down due to the internal liquid electrolyte absorbing spin energy.

The four independent measures of the MAA spin rate were plotted versus mission elapsed time in days and fit with an exponential function. The results are shown in Fig. 11, with a decay constant of -0.189.

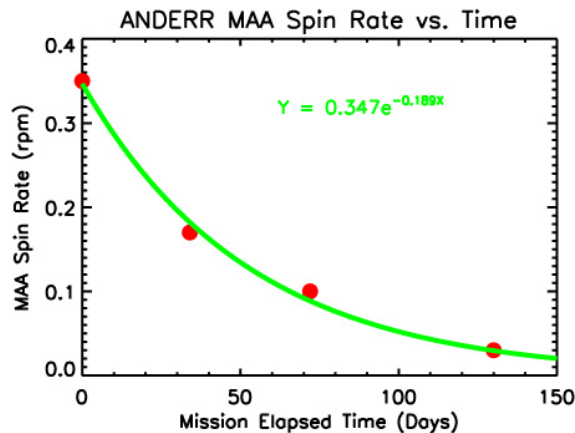


Fig. 11. MAA spacecraft spin rate decay.

### 3. ATMOSPHERIC CORRECTIONS

The NRL Orbit Covariance Estimation and Analysis (OCEAN) [14] orbit determination code version 5.01 was configured to make weighted least squares estimates of the initial (beginning in the middle of a day) and the fit and prediction final ephemeris was produced. The observation data were corrected for known biases (and center of mass) and weighted using past sensor performance values so that the SLR data naturally biases the solutions toward reality in the hybrid SSN and SLR runs. The high fidelity force models including either EGM-96 or GGM02C at degree and order 70x70, the ocean tides, the MSIS density models, the HWM93 thermospheric winds, and all IERS conventions frames and displacement typical for accurate SLR processing.

A comparison between the resulting MAA  $C_D$  and FCal  $C_D$  from the OCEAN run, using MSISE and a priori area and mass information, yields very little difference between the two objects as seen in Fig. 12. The average  $C_D$  value for MAA is 1.690 with a standard deviation of 0.1557. The average  $C_D$  value for FCal is 1.676 with a standard deviation of 0.1703. These results are clearly non-physical, as the value is well below 2.0. The MSIS model is over-

estimating the atmospheric density by about 25% on average and the OCEAN code is correcting for this by scaling the B term down. This over-estimation of the thermospheric density is in direct agreement with the findings of Emmert and Picone [15]. The average ratio for MAA is 80.2% with a standard deviation of 7.46% and the average ratio for FCal is 79.5% with a standard deviation of 8.1%.

The observations were also processed using the Jacchia 70 (J70) model atmosphere. The results are plotted against the MSIS results in Figure 12. The average  $C_D$  value for  $MAA_{J70}$  is 1.727 with a standard deviation of 0.2483. The average  $C_D$  value for  $F_{Cal_{J70}}$  is 1.720 with a standard deviation of 0.2755. The average value is closer to theory but the scatter is 59% larger for the MAA and 62% larger for FCal when using J70 instead of MSIS.

The primary drivers of the atmosphere are solar radiation heating and geomagnetic heating. These drivers have inputs into MSIS and J70 in the form of the F10.7 cm radio flux, a proxy (due to its ease of measurement on the ground) for the solar ultraviolet flux that heats the atmosphere. The  $A_p$  and  $k_p$  indices are a measure of geomagnetic activity at the Earth and are used by atmospheric models to drive the geomagnetic heating in the atmosphere. Fig. 12 plots the OCEAN fitted  $C_D$  values against both the daily F10.7 cm flux and the daily index. There is a slight trend

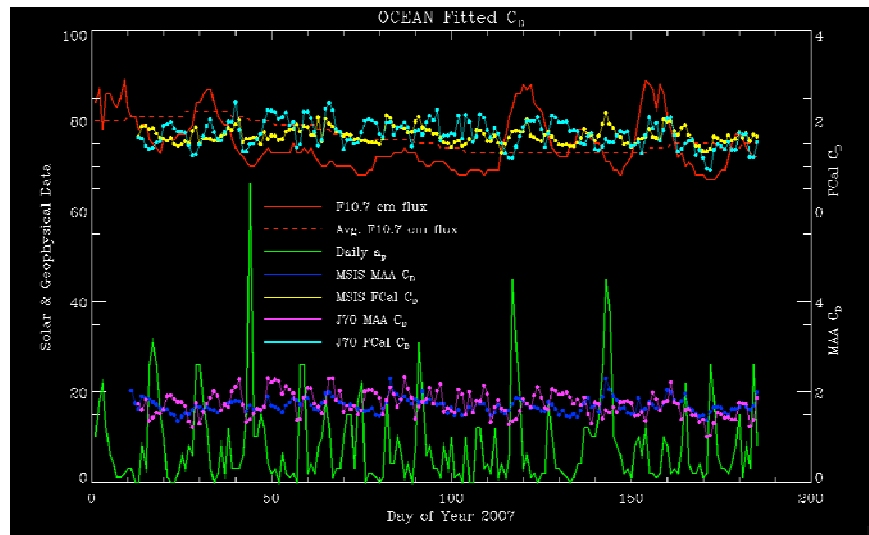


Fig. 12. OCEAN fitted  $C_D$  values, using NRL MSISE2000 for the MAA (blue) and FCal (yellow) spacecraft; using NRL Jacchia 70 for the MAA (purple) and FCal (light blue) spacecraft, with the solar f10.7 cm flux (red) and the daily average  $A_p$  geomagnetic index (green).

with the F10.7 cm flux values, which may be indicative that the temperature in the atmospheric models is incorrect and over-estimating the atmospheric density. There is clear correlation that the geomagnetic activity, even at these relatively low levels of geomagnetic activity, is not being completely accounted for in the MSIS or J70 models. Latency in the  $C_D$  values with response to the geomagnetic activity is expected (and observed) due to the timescales that the atmosphere responds to the geomagnetic forcing.

For fit-spans that are much longer than the timescale of an objects variations in  $B$  one can state the relationship between two objects  $i$  and  $j$  as

$$\frac{B_i^T}{B_j^T} = \frac{B_i^M}{B_j^M} \quad (4) \quad B_i^T = B_i^M \frac{C_{D_{maa}}^T}{C_{D_{maa}}^M} \quad (5)$$

where  $B^T$  represents the true value of  $B$  and  $B_M$  is the modeled, or fitted, value. Due to the inherent symmetry of the ANDERR spacecraft, the frontal area ( $A$ ) is well characterized and remains constant independent of orientation and the mass ( $m$ ) is constant for both the ANDERR MAA and the FCal spacecraft. Hence, Eq. 4 may be re-written as Eq. 5 using the ratio of MAA  $C_D$  values, true over modeled, as a calibration correction which can be applied to obtain  $B^T$  of an independent object  $i$ .

The practical impact of having a correctly scaled thermospheric density was measured by comparing the 24-hour prediction revolution to the reference ephemeris. This was constructed by establishing a time series of scale factors required to rescale the recovered  $C_D$  from the OCEAN fit using the MSIS atmospheric model over a 3 day fit interval on the MAA spacecraft. These scale factors were applied to each unique day (multiple scalings occur during the testing fit and prediction interval) and do include scaling on the prediction interval (posterior knowledge was utilized). Results are plotted in Fig. 13, the  $C_D$  values are flat over the time series and do not show a correlation with the atmospheric drivers.

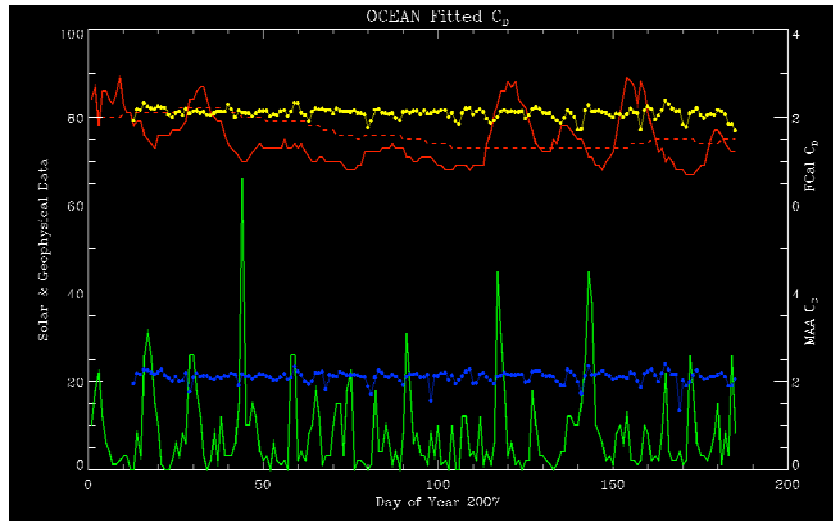


Fig. 13. Daily scaled OCEAN fitted  $C_D$  values, using NRL MSISE2000 for the MAA (blue) and FCal (yellow) spacecraft; with the solar f10.7 cm flux (red) and the daily average Ap geomagnetic index (green).

The comparison is a measure of the in-track bias measured over one orbit period at the end of the first day of prediction. This is constructed from time of day and not last dataset, and may be measuring more than just a 24 hr prediction, as the observation data is not uniformly available on a target of this altitude. Both the FCal and the MAA were generated with this process (using the MAA's rescale factor).

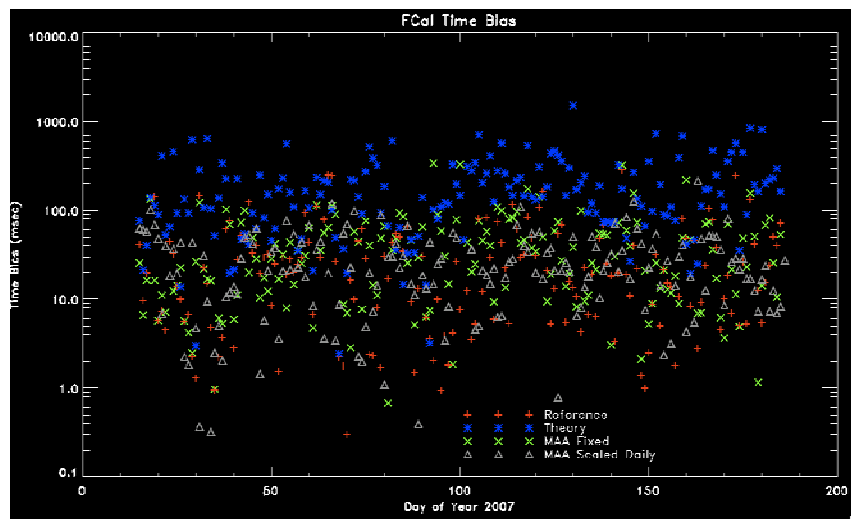


Fig. 14. In-track time bias of the FCal spacecraft predictions at 24 hours. Allowing B to float (red), Fixing B to theory (blue), scaling B with average MAA results for the 6-months (green), scaling B with daily MAA results (grey).

A comparison of the in-track time bias, the time difference between where the predicted object location and the actual location, is used as a performance metric for four different OCEAN fits using NRL MSISE2000 as the atmospheric model. Four cases were processed for FCal using information from a 48-hour fit of MAA as the reference object. First the FCal data were processed allowing the B term to float, or be scaled by OCEAN. The second case was to fix the B term to the theoretical value using 2.1088 as the  $C_D$ . The third process fixed the B term to the six-month average MAA value. The last case scaled the B term daily as described by Eq. 5. The results are plotted as Fig. 14 at the 24-hour mark and the means and standard deviations are presented in Table 1. Using the daily MAA scale factors shows a marked improvement in the mean (15.2%) and the standard deviation (39.9%) over the reference method.

Table 1. FCal In-Track Time Bias (msec)

	Reference	Theory	Scaled Fixed	Scaled Daily
Mean	35.43	202.82	45.40	30.05
Std. Dev.	47.33	200.49	53.69	28.46

#### 4. CONCLUSIONS

It is clear that the ANDERR spacecraft are useful calibration targets due to their well-characterized size and shape. The spin rate was measured by four independent methods, which are all consistent with an exponential decay of the MAA spin rate. These data are vital to the design of the follow-on ANDE spacecraft now in progress. The SLR observations performed by the members of the ILRS have been used to augment the radar data to constrain the accuracy and stability of the estimated ballistic coefficient and to assess the accuracy of the predictions with absolute confidence. The data show a consistent over estimation of the density by the atmospheric models, MSIS as well as J70. The average in-track time bias at the 24-hour mark improved by 15.2% with a 39.9% improvement in standard deviation. While the average fitted  $C_D$  for J70 was closer to the analytic value, the MSIS  $C_D$  values have considerably less variation. The over specification of total density is in agreement with the findings of Emmert and Picone [15], who have shown a consistent decrease in thermospheric density of the past three decades. The models are having a difficult time properly capturing the effect of geomagnetic forcing (especially at low end of the solar/geomagnetic forcing range), as correlations are evident in the fitted  $C_D$  values with the geomagnetic  $A_p$  index. The ANDERR data set is extensive and the objects are not expected to decay until December, 2007 (MAA) and April 2008 (FCal). We expect to continue this work over the entire mission duration, and apply the corrections to other objects. Work will also focus on short arc studies, 1/4 to 1/2 of an orbit where geometric solutions have been collected.

#### 5. FUTURE WORK

Atomic oxygen (O), the major constituent of the Earth's thermosphere above 200 km altitude is both a driver and a tracer of atmospheric motions in the thermosphere and plays a pivotal role in interactions with the ionosphere through ion-drag and chemical reactions. Satellites in low-Earth orbit require knowledge of O densities to address engineering issues in low-Earth-orbit missions. The major difficulties in O measurements involve ambiguities due to the recombination of O in the sensor surfaces to yield  $O_2$ , which is then measured with a mass spectrometer; similar difficulties exist for atomic hydrogen H and nitrogen N.

A follow-on ANDE mission is scheduled for April 2009. This mission will consist of two 19-inch diameter spherical spacecraft, each fitted with retro-reflectors. One of the spacecraft will carry onboard instrumentation designed to simultaneously measure thermospheric density, composition and winds at the spacecraft location. This new miniaturized charged particle spectrometer is capable of measuring relative densities and energies of the neutral and ion constituents in the upper atmosphere. Neutral atoms are ionized before striking internal surfaces and accommodated atoms and molecules are discriminated from incident ones according to their energies. The ion source sensitivity is about  $1.3 \times 10^{-4}$ /s per microAmp electron beam current for a number density of  $1/\text{cm}^3$ ; operating with 1 mA emission (about 0.2W cathode power), signals of 100/s with integration period of 1 second correspond to a neutral atom density of about  $10^3/\text{cm}^3$  with 10% variance. Total power for the spectrometer is less than 0.5 W with a mass of about 0.5 kg.

The active spacecraft will also carry an optical communications experiment. The NRL modulating retro-reflector (MRR) system consists of an optical retro-reflector coupled with a multiple quantum well (MQW) electro-optic shutter [16,17]. When a low voltage (on the order of 5V) is applied to the MQW device, the shutter is open allowing

photons from the interrogation beam to enter the system. The photons are then reflected back along the original angle of incidence by the retro-reflector. The electronic driver encodes the data to be transmitted, which is modulated by the MQW device, resulting in a modulated return beam carrying the data stream. This system provides a compact, low power (<50 mW per device), asymmetric optical communication platform. The Field-of-View (FOV) of a typical mounted device is of the order of 26 degrees (far field) and the operation wavelengths for the NRL units can be 980 nm or 1.06  $\mu\text{m}$ , or 1550nm. The active sphere will have a predetermined pattern of MRRs distributed over the sphere. For this experiment, the system's nominal data transmission rate will be between a few bits per second and  $\sim 10$  kbps. The ground site intended for use in the MRR communications experiment is the NRL Midway Research Center in near Quantico, VA.

## 6. ACKNOWLEDGEMENTS

We would like to acknowledge the Department of Defense Space Test Program for their support in the ANDERR mission. We would also like to acknowledge the ILRS for acquiring routine laser ranging data for both of the ANDERR spacecraft. We acknowledge the Air Force Research Laboratory Det. 15 for acquiring photometric observations of the MAA spacecraft.

## 7. REFERENCES

1. A.C. Nicholas, et al., "The Atmospheric Neutral Density Experiment (ANDE)" *Proc. of the 2002 AMOS Technical Conference*, Maui HI, Sept. 2002.
2. A.C. Nicholas, G.C. Gilbreath, S.E. Thonnard, R.A. Kessel, R. Lucke, C.P. Sillman. "The atmospheric neutral density experiment (ANDE) and modulating retroreflector in space (MODRAS): combined flight experiments for the space test program" *Proc. SPIE* Vol. 4884, p. 49-58, Optics in Atmospheric Propagation and Adaptive Systems V; Anton Kohnle, John D. Gonglewski; Eds., March 2002.
3. A.C. Nicholas, S. Thonnard, I. Galysh, P. Kalmanson, B. Bruninga, H. Kelly, S. Ritterhouse, J. Englehardt, K. Doherty, J. McGuire, D. Niemi, H. Heidt, M. Hallada, D. Dayton, L. Ulibarri, R. Hill, M. Gaddis, B. Cockreham, "An Overview Of The ANDE Risk Reduction Flight", *Proc. of the AMOS Technical Conference*, Maui, HI, Sept. 2002.
4. D. Vallado, and S. Carter, "Accurate Orbit Determination from Short-Arc Dense Observational Data", *Proc. of the AAS/AIAA Astrodynamics Specialist Conference*, Paper AAS 97-704, Sun Valley, Idaho, Aug 4-7, 1997.
5. A. C. Nicholas, J. M. Picone, J. Emmert, J. DeYoung, L. Healy, L. Wasiczko, M. Davis, C. Cox, "Preliminary Results from the Atmospheric Neutral Density Experiment Risk Reduction Mission", *Proc. of the AAS/AIAA Astrodynamics Specialist Conference*, paper #AAS 07-265, Mackinac Island, MI, Aug 20-24, 2007.
6. L. Jacchia, "New Static Models of the Thermosphere and Exosphere with Empirical Temperature Profiles," *Smithsonian Astrophys. Observatory Special Rep.* No. 313, May 6, 1970.
7. A.E. Hedin, "MSIS-86 Thermospheric Model," *J. Geophys. Res.*, 92, 4649-4662, 1987.
8. A.E. Hedin, "Extension of the MSIS Thermosphere Model Into the Middle and Lower Atmosphere," *J. Geophys. Res.*, 96, 1159-1172, 1991.
9. J. M. Picone, A. E. Hedin, D. P. Drob, and A. C. Aikin, "NRLMSISE-00 Empirical Model of the Atmosphere: Statistical Comparisons and Scientific Issues," *J. Geophys. Res.*, (2001).
10. C.M. Cox and F.G. Lemoine, Precise Orbit Determination of the Low Altitude Spacecraft TRMM, GFZ-1, and EP/EUVE Using Improved Drag Models, *Proc. of the AAS/AIAA Space Flight Mechanics Meeting*, Paper AAS 99-189, Breckenridge, Colorado, February, 1999.
11. E.D. Knechtel and W.C. Pitts, Normal and Tangential Momentum Accomodation for Earth Satellite Conditions, *Astronautica Acta*, Vol. 18, 1971.
12. A.E. Hedin, E. L. Fleming, A. H. Manson, F. J. Schmidlin, S. K. Avery, R. R. Clark, S. J. Franke, G. J. Fraser, T. Tsuda, F. Vial, and R. A. Vincent, "Empirical Wind Model for the Upper, middle and Lower Atmosphere", *J. Atmos. Terr. Phys.*, 58, 1421-1447, 1996.
13. M. R. Pearlman, Degnan, J.J., and Bosworth, J.M., "The International Laser Ranging Service", *Advances in Space Research*, Vol. 30, No. 2, pp. 135-143, July 2002.
14. M. Soyka, J. Middour, P. Binning, H. Pickard, J. Fein, "The Naval Research Laboratory's Orbit / Covariance Estimation and Analysis Software: OCEAN", *Proc. of AAS/AIAA Astrodynamics Meeting*, pp1567 - 1586, Sun Valley, Idaho, 1997.

15. Emmert, J. T., J. M. Picone, J. L. Lean, and S. H. Knowles, Global change in the thermosphere: Compelling evidence of a secular decrease in density, *J. Geophys. Res.*, 109, A02301, doi:10.1029/2003JA010176, 2004.
16. G. C. Gilbreath, W. S. Rabinovich, T. J. Meehan, M. J. Vilcheck, R. Mahon, Ray Burris, M. Ferraro, I. Sokolsky, J. A. Vasquez, C. S. Bovais, K. Cochrell, K.C. Goins, R. Barbehenn, D. S. Katzer, K. Ikossi-Anastasiou, and Marcos J. Montes, "Large Aperture Multiple Quantum Well Modulating Retroreflector for Free Space Optical Data Transfer on Unmanned Aerial Vehicles", *Opt. Eng.*, 40 (7), pp. 1348-1356.
17. G.C. Gilbreath, S.R. Bowman, W.S. Rabinovich, C.H. Merk, H.E. Senasack, "Modulating Retroreflector Using Multiple Quantum Well Technology", *U.S. Patent No. 6,154,299*, awarded November, 2000.